Journal of Materials Research and Technology 36 (2025) 2951–2959

Contents lists available at ScienceDirect

Journal of Materials Research and Technology

journal homepage: www.elsevier.com/locate/jmrt

Fatigue life enhancement via residual stress engineering due to local forming during refill friction stir spot welding

Niklaas Becker [a,*], Daniel Kuhn [b], Jan Piochowiak [b], Benjamin Klusemann [a,c]

[a] Helmholtz-Zentrum Hereon, Institute of Materials Mechanics, Solid State Materials Processing, Max–Planck-Straße 1, 21502 Geesthacht, Germany
[b] Siemens Mobility GmbH, Duisburger Straße 145, 47829 Krefeld, Germany
[c] Leuphana University of Lüneburg, Institute for Production Technology and Systems, Universitätsallee 1, 21335 Lüneburg, Germany

ARTICLE INFO

Keywords:
Refill friction stir spot welding
Fatigue life
Residual stress
AA6005A-T6

ABSTRACT

Refill friction stir spot welding is a promising joining process in lightweight design. As lightweight structures react sensitively to cyclic loads, the fatigue life of the joints are of particular interest. In previous studies, attempts have been made to optimize the fatigue properties based on process parameter modification albeit with moderate success. The introduction of post-processing steps such as laser-shock or hammer peening resulted in an improvement but also in a considerable higher effort. In this work, a new approach is pursued, namely to increase the fatigue life properties by manipulating the residual stresses already during the welding process. This is achieved by milling a pocket into one of the joining surfaces prior to the welding process. The pocket and the clamping forces that occur during the welding process cause an elongation of the material. After releasing the clamping force, the elastic springback effect causes compressive forces, leading to compressive residual stresses in the spot weld. This has made it possible to increase the endurance limit for shear-loaded samples by a factor of 40 and for cross-tension-loaded samples by a factor of 18.

1. Introduction

As environmental protection will be the task of the next generations, issues such as sustainability are becoming increasingly important. Sustainability means reducing the weight of all types of vehicles and at the same time designing them in such a way that they can remain in service as long as possible. Solid-state joining processes are considered particularly sustainable among other welding processes, as they not only use 42% less energy and 10% less material compared to gas metal arc welding [1], but are also suitable for welding high-strength aluminum alloys [2]. The best-known solid-state joining process is probably friction stir welding (FSW), which produces a linear weld seam. However, since spot-wise joining is often sufficient for structural applications, friction stir spot welding (FSSW) and refill friction stir spot welding (refill FSSW) are frequently used. Refill FSSW has significant advantages over FSSW in terms of strength and surface quality [3] and is therefore seen as a potential successor of resistance spot welding and riveting in the automotive and aircraft industries [4]. In order to obtain the optimum strength from refill FSSW, several process parameter optimization studies have already been carried out on various structural aluminum alloys. For example, Kubitz et al. [5] performed a quasi-static process parameter optimization for AA7075-T6 and identified that too low temperature leads to poor bonding while too high temperature leads to unfavorable microstructural properties. Zhou et al. [6] conducted a comparable study for AA6061-T6 and came to very similar conclusions. Whereas Tier et al. [7] investigated the influence of the welding parameters on the microstructure of AA5042 and the resulting shear strength and came to the conclusion that the process parameters with the greatest influence on the shear strength are the plunge depth followed by the rotation speed. For AA2024, Li et al. [8] examined the mechanical properties as a function of the rotation speed and found that with increasing rotation speed, the grain size in the SZ increases and the width of the bonding ligament decreases, resulting in a decrease in strength.

However, such studies are mainly limited to static properties, but one of the biggest challenge in automotive and aircraft industries, where structural aluminum alloys are mainly used, is the high cycle fatigue performance. In this context, studies have been already carried out with the aim of increasing fatigue performance, but the results were unsatisfactory so far. For instance, Lage et al. [9] carried out a quasi-static optimization of the welding parameters for AlMgSc alloys and then examined these parameters with dynamic conditions, where the dynamic target of 10^6 cycles was achieved at only 9% of the static shear strength. Similarly, Effertz et al. [10] did comparable investigation for

* Corresponding author.
E-mail address: niklaas.becker@hereon.de (N. Becker).

https://doi.org/10.1016/j.jmrt.2025.03.205
Received 15 January 2025; Accepted 23 March 2025
Available online 3 April 2025

AA7050-T76 with reaching only 10% of the static loads and suggesting that the material is not recommendable for high load cyclic application.

In this regard, a quasi-static process parameter optimization led to insufficient fatigue results, as the failure mechanisms of quasi-static and dynamic failure simply differ, i.e. the optimal process parameters for quasi-static properties might not represent the optimal ones for the fatigue performance. However, optimizing welding parameter with regard to fatigue performance is much more complex than for quasi-static performance, hence the literature on this subject is limited. Anyway, in order to understand the failure of refill FSSW joints under high cycle loads, attention must be paid not only to the microstructure, but particularly to residual stresses. Becker et al. [11] investigated crack propagation in refill FSSW and showed that fatigue cracks could be deflected due to residual compressive stresses. Similar effects have also been observed in FSW welds, for example, Pouget et al. [12] observed the influence of residual stresses and microstructure on fatigue cracks in friction stir welds and concluded that the influence of residual stresses outweighs the influence of the microstructure. Ma et al. [13] showed in their work on fatigue crack growth in FSW seams that it was difficult to initiate cracks at all in areas where compressive stresses were present. There are also approaches in which the microstructure and residual stresses are influenced in a targeted manner during the welding process, for example, friction stir vibration welding (FSVW). In this process, the sample is brought to oscillate by a special device during the welding process. As Bagheri et al. [14] were able to show for FSSW, this has an influence on the microstructure, in particular it leads to smaller grain size and to a change in the residual stress distribution within the weld. Whereas Wu et al. [15] compared the fatigue life properties of FSW and FSVW and found that FSVW can be used to increase the fatigue life of the welded joints.

This brief literature overview proves that residual stresses have a major influence on the fatigue life of solid-state joining processes. In this regard, this study investigates the change of the residual stress state by geometric changes to the joining partners and outlines the significant effect on fatigue life. The presented novel approach has the advantage of improving the fatigue life without an additional process step, such as laser shock- or hammer peening.

2. Materials and methods

2.1. Material and welding

The material used for this study was taken from an extruded hollow chamber profile made of AA6005A-T6 with a wall thickness of 3.2 mm, reflecting industrial application scenarios. The sample geometry, see Fig. 1, was cut out using water jet cutting, where the long axis of the sample corresponded to the direction of extrusion, and milled to a thickness of 3.0 mm. Pockets with a diameter 25.0 mm, and a depth of 0.3 mm were milled into the lower joining partner of the modified samples.

The samples were welded on a refill FSSW machine RPS100 (Harms & Wende, Germany). The three-part tool used is made of Hotvar alloy and has the following diameters: Clamping ring: 17 mm; Shoulder: 9 mm; Probe: 6 mm. The welding process is performed in its shoulder-plunging variant using the process parameters: Rotation speed (Rs): 1500 rpm; Plunge depth (Pd): 3.1 mm; Plunge time (Pt): 1.5 s; Clamping force (Cf): 8.0 kN. Since the failure of the cross tension specimen (CTS) under cyclic load was initially observed in the area of the lack of refill, as will be discussed later, an underfill of 0.2 mm was used to avoid this defect, see Fig. 2 (c). As failure in the lap shear specimens (LSS) did not occur in the area of the spot weld, but in the base material, this process adjustment was not performed in case of the LSS specimens. In the modified samples, the sheet with the pocket was always positioned at the bottom of the overlap configuration.

2.2. Fatigue tests

The fatigue tests were carried out at room temperature on servo hydraulic testing machines (Schenk, Germany) with a maximum force of 10 kN. Six load levels with five specimens each were tested for each Wöhler curve. All tests were performed with a load ratio R = 0.1 at a frequency f = 20 Hz. The following load levels were selected for the lap shear specimens $F_{max}[N]$: 2730; 2390; 2090; 1830; 1600; 1400. The cross tension specimens were tested at $F_{max}[N]$: 1896; 1422; 1067; 800; 600; 450. The endurance limit was defined as 10^7 cycles.

The modified samples were tested at two load levels with at least 3 samples each. For the modified lap shear specimens, the load levels were $F_{max}[N]$: 3110 and 4060. The modified cross tension specimens were tested at $F_{max}[N]$: 1422 and 1067.

2.3. Microstructure and hardness

For metallographic analyses, the samples were prepared as follows: Cutting the sample near the center, embedding in polymer resin, grinding, polishing and etching in Barker solution using a Struers LectoPol-5 with 25 V for 90 s.

The microstructure analysis was performed with an FEI Quanta 650 scanning electron microscope (SEM) equipped with an electron backscatter diffraction (EBSD) system. The measuring area was scanned with a step width of 0.2 μm in X- and Y-direction at a voltage of 20 kV.

The hardness was measured via a Struers Durascan by a Vickers indenter with an opening angle of 136° using the HV0.1 method. The distance between the measuring points is 0.25 mm in X- and Y-direction.

2.4. Residual stress

Residual stresses within different CTS samples were measured in transmission using high-energy X-ray diffraction at beamline P07B at DESY (Deutsches Elektronen Synchrotron, Hamburg, Germany). An area of 50 × 50 [mm] was measured with a horizontal and vertical measurement distance of 1.0 mm, see Fig. 1. The Al (311) reflection was used to evaluate the strains in X- and Y-direction with the help of the software pydidas. Since the surface of the modified specimens is deformed, a peak correction must be carried out, which was done using copper paste.

3. Results

3.1. Microstructure and hardness analyses

At first, the microstructure of the spot welds performed by refill FSSW was investigated. Fig. 2 (a) shows a defect-free spot weld in which the characteristic microstructural zones of refill FSSW are shown: stir zone (SZ), thermomechanically affected zone (TMAZ) and heat affected zone (HAZ). The microstructure of a modified sample is presented in Fig. 2 (b), where geometric defects such as the so-called lack of refill and voids between the SZ and the TMAZ can be seen. Both of these defects indicate incomplete refilling, i.e. there is not enough material for faultless refilling. The material that is plasticized during the welding process is pressed by the tool into the gap between the two sheets, which is created by the pocket in the modified specimen. As the escaping of the material cannot be prevented, the offset of the tool was changed by 0.2 mm. Although this results in a defect on the surface of the spot weld, i.e. an underfill, Fig. 2 (c), it prevents the more serious defects of lack of refill and formation of voids. Furthermore, the deformation of the modified specimen caused by the pocket can be observed, Fig. 2 (b), (c). Fig. 2 (d) presents the hook region of the reference sample, which is also considered to be particularly relevant in terms of strength of the weld but, unlike friction stir lap welding (FSLW) [16], does not depend on the thermodynamic conditions during

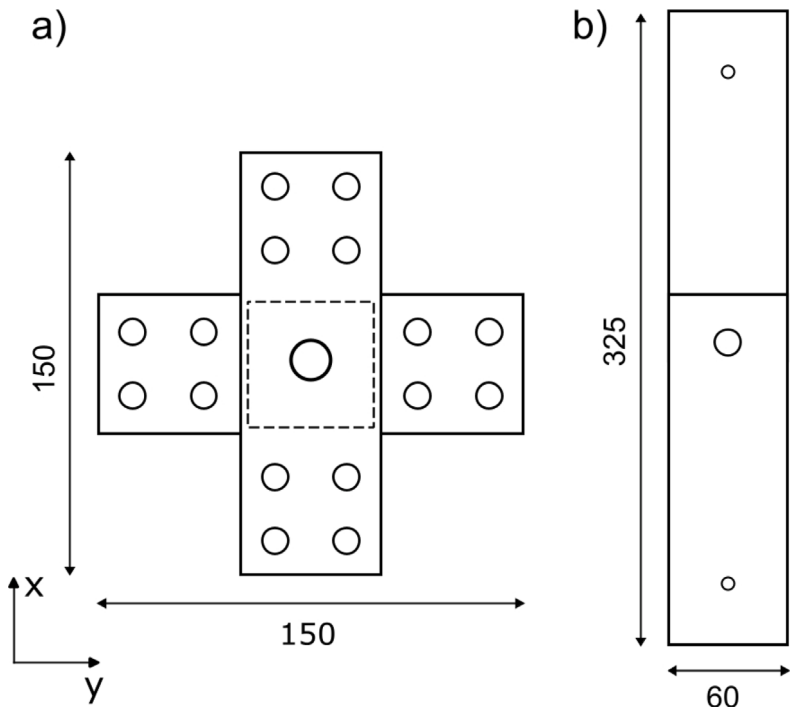

Fig. 1. Specimens geometry according to ISO 14324. (a) Cross-tension fatigue test specimen (CTS); (b) Lab shear fatigue test specimen (LSS). The dashed square on the CTS marks the area of the residual stress measurement. All dimensions in [mm].

the welding process rather on the plunge depth [17]. The shape of the hook here can be described as a flat hook, which is a mediocre hook formation in terms of strength [17]. Due to the lack of refill in case of the modified sample, no hook appears, Fig. 2 (e). In Fig. 2 (f) the modified sample with 0.2 mm underfill is shown, where an upward pointing hook has formed, which is known in the literature as typically strength-reducing [17].

Fig. 3 shows the results of the texture analysis. Both measurements in the center of the spot welds show a moderate, symmetrical shear texture with no major differences in intensity. However, at a distance of 3.5 mm from the weld center the shear texture is very pronounced in the reference specimen, Fig. 3 (h), where it is much less significant in the modified specimen, Fig. 3 (i). Outside the spot weld at 5.5 mm, a texture typical for extrusion is present, where no significant differences are recognizable between both samples.

The observed shear texture is caused by the rotation of the tool, however, in case of the modified specimen the texture is less pronounced due to elastic springback resulting from the local forming during the welding process. At the beginning of the welding process, the clamping ring applies the clamping force and as consequence the upper sheet is deformed until it rests against the surface of the pocket of the lower sheet. After completion of the welding process the sheets are joined and the clamping ring is removed, therefore elastic springback occurs. The elastic springback and the consequential tensile load in Z-direction leads to an axial alignment of the grains [18]. Furthermore, since the material in the spot weld is still at an elevated temperature, recrystallization is probably not yet complete [19], which facilitates the reorientation of grains. The shear texture, which is a result of the welding process, is superimposed by the axial alignment of the grains, which is caused by the elastic springback, and is thus significantly reduced.

The hardness distribution shows the typical W-shape for precipitation-hardenable aluminum alloys after solid-state processing [20], see Fig. 4. Softening takes place within the spot weld due to the dissolution of β'' precipitates [21]. However, the hardness gradient hardly differs between the reference specimen and the modified specimen. Only the HAZ in the modified specimen is slightly larger in the upper sheet, which can be attributed to the lower heat dissipation through the pocket.

3.2. Fatigue tests

Fig. 5 (a) shows the fatigue results of the lap shear specimens, comparing the results of the reference specimens with those of the modified specimens. The results are significant improved for the modified specimens. For instance, the number of cycles at a load of 3.0 kN is increased from 250,000 to 10,000,000. The modified specimens still reach the endurance limit of 10^7 cycles with a maximum load of 2990 N, where the reference specimens only reached the endurance limit with a maximum load of 930 N.

The cross tension fatigue results are displayed in Fig. 5. It can be observed that the modified specimens have slightly better fatigue life results than the reference specimens, however, the improvement is significant less compared to the LSS. This is related to the deteriorating effect of the occurring defects in the modified specimens, which reducing the observed fatigue improvement of the LSS in case of the CTS. However, by changing the tool offset to produce a 0.2 mm underfill, avoiding the lack of refill, this increases the fatigue performance of CTS also significantly, see Fig. 5 (b).

For instance, the number of cycles at a load of 930 N increases from 535,000 for the reference specimens to 10,000,000 for the modified specimen with 0.2 mm underfill. The modified specimen with underfill reaches the endurance limit of 10^7 cycles at a maximum load of 930 N instead of 125 N for the reference specimen. For higher loads, this improvement is not so drastic, as the effect of residual stress decreases and other effects such as underfill increases, as will be discussed in Section 4.

Fig. 6 shows the crack paths in the LSS and CTS specimens. For the reference sample, Fig. 6 (a), the crack path appears as expected for refill FSSW under cyclic shear loading [22]. The nucleus of the crack occurred at the end of the hook and then propagated horizontally through the sample. In contrast, for the modified specimen the crack nucleated at the notch of the pocket in the base material from where it propagated horizontally through the specimen, Fig. 6 (b).

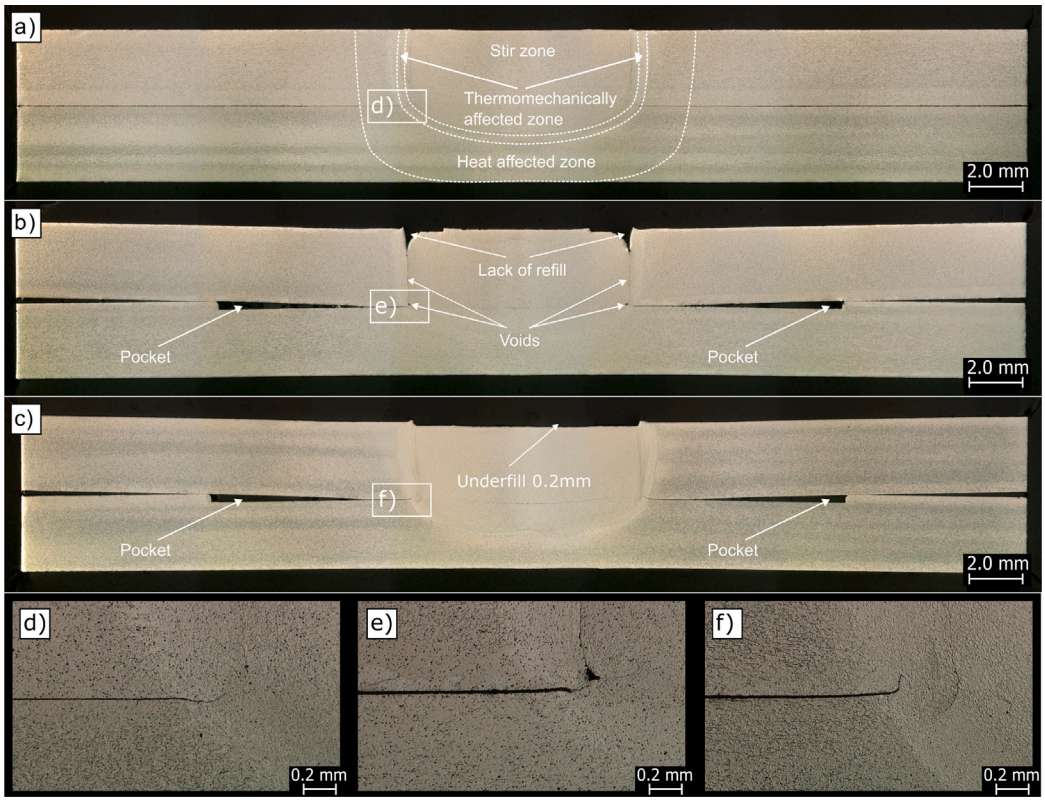

Fig. 2. Microstructure of (a) reference specimen, (b) modified specimen, (c) modified specimen with 0.2 mm underfill. Hook in (d) reference specimen, (e) modified specimen, (f) modified specimen with 0.2 mm underfill.

The fact that the crack in the modified LSS sample nucleated in the base material and not in the area of the hook implies that compressive stresses might be present here. The conditions for crack nucleation in the area of the hook are favorable due to a multitude strength-reducing effects: the notch between the weld components (hook), the cross-sectional tapering due to the volumetric defects, the low strength of the HAZ and the strength mismatch between SZ and TMAZ. On the other hand, there is only the reduction in cross-section and the notch of the pocket at were the crack nucleation in the base material.

In case of the modified CTS specimen, a classical pull-out is observed, Fig. 6 (c), which is related to the lack of refill. This can be changed by applying the 0.2 mm underfill, where the crack followed the HAZ and thus propagated in the lower sheet, Fig. 6 (d).

3.3. Residual stress

Residual stresses in refill FSSW are caused due to the thermo-mechanical processing. The largest proportion of residual stresses arises from the temperature gradient generated by friction between the tool and the workpiece [23]. The friction generates heat, which causes the material to expand, resulting in residual compressive stresses outside the recrystallized area of the spot weld. As soon as the welding process is complete and dynamic recrystallization is concluded, residual tensile stresses occur within the spot weld. These result on the one hand from the preceding plastic deformation and on the other hand from the fact that the heated material cools down but is hindered in its contraction by the surrounding material [24].

Fig. 7 shows the residual stresses of the reference specimen and the modified specimens. As the sheets were extracted from extruded profiles, no homogeneous stress distribution can be observed over the measurement area, but being representative for actual industrial application. However, the amount of these initial residual stresses can be neglected for the current investigation and are considerable smaller in comparison to the stresses due to the spot welding process.

The typical residual stress profile of refill FSSW can be seen for the reference specimen Fig. 7 (a), (b). This is characterized by strong residual tensile stresses within the spot weld. However, in the modified samples Fig. 7 (c), (d), the residual stress profile looks different, where the residual stresses are lower overall. Although tensile residual stresses continue to exist outside and in the middle of the weld spot, stress neutrality prevails in the transition region between SZ and TMAZ. Since fatigue cracks nucleate in the area of the transition region in conventionally executed refill FSSW [25], see also Fig. 6 (a), it is particularly preferable not to have tensile residual stresses in the transition region.

4. Discussion

It is well accepted in the literature that in particular the microstructure (including typical features, defects and strength) and residual stresses are decisive for the fatigue behavior of friction stir-welded joints [26]. However, contradictory observations are reported in terms of which factor has the greatest influence. In this study, these factors were compared via the reference specimen and the modified specimen in the previous section. In terms of strength, investigated via hardness, no significant differences could be detected, see Fig. 4. Although significant defects occurred in the modified samples, better fatigue results were achieved, i.e. defects seem not significantly responsible for the fatigue properties for the welded samples. This is in contradiction to the literature, where these defects are described as deteriorating the fatigue properties [27]. Although the characteristic of the hook, which is described in the literature as the feature with the greatest influence on the mechanical properties of refill FSSW joints [28], is particularly unfavorable in the modified sample with the 0.2 mm underfill, the fatigue properties are even better compared to the reference sample. Therefore, the characteristic of the hook can also be excluded as the reason for the improved fatigue life results.

The EBSD analysis shows that the modified samples have smaller grains and a weaker texture intensity within the recrystallized area

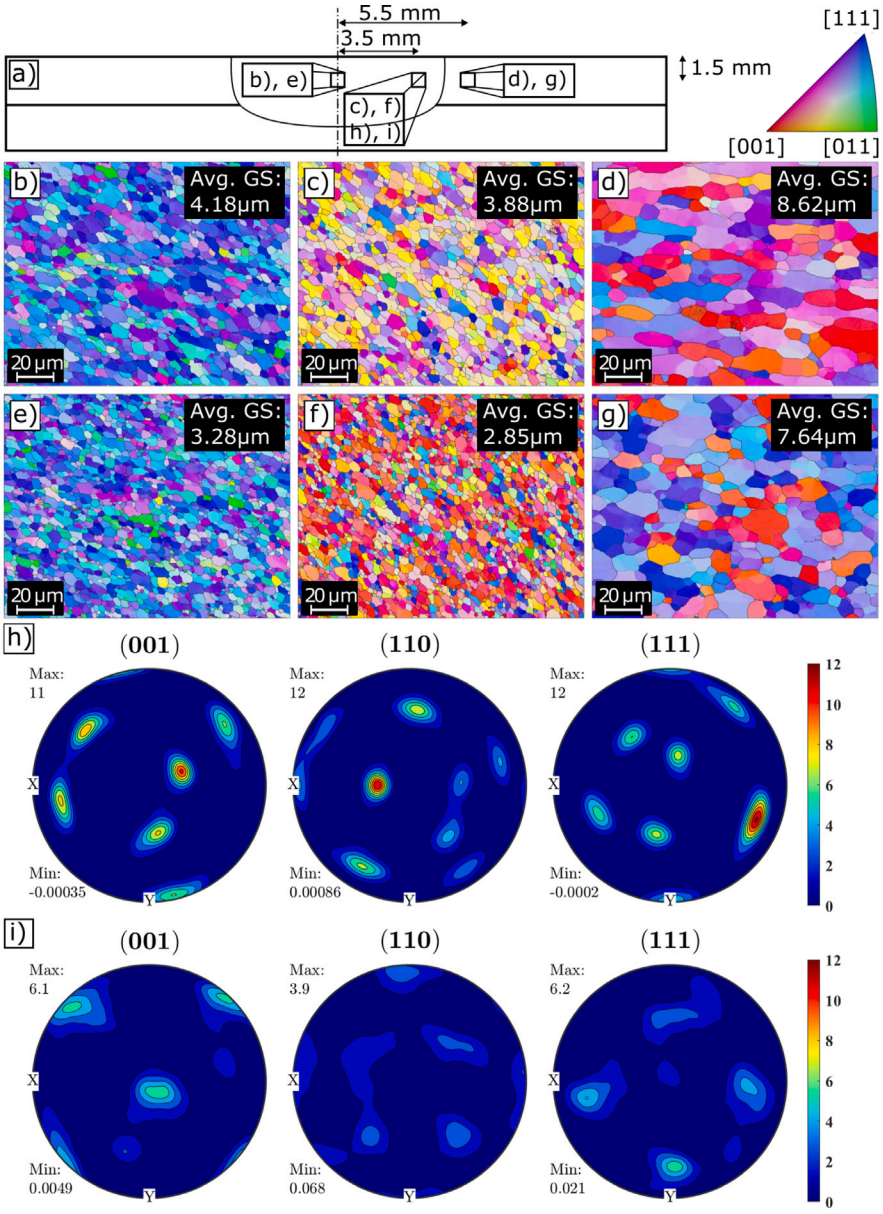

Fig. 3. (a) Sketch of measurement positions for EBSD analyses; IPF of reference sample in (b) the center, (c) at 3.5 mm, (d) at 5.5 mm; IPF of modified sample in (e) the center, (f) at 3.5 mm, (g) at 5.5 mm; Pole figures of (h) reference sample and (i) modified sample at 3.5 mm.

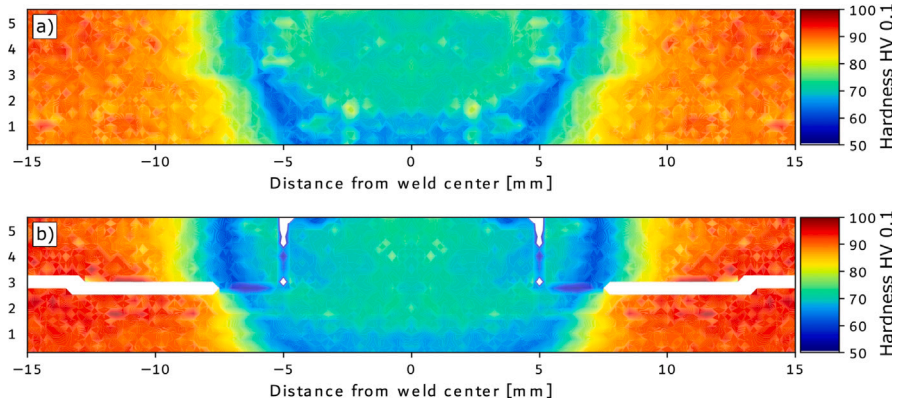

Fig. 4. Hardness distribution of (a) reference specimen and (b) modified specimen. No reliable hardness values could be measured within the white areas of the modified specimen, as not sufficient material is present in these areas.

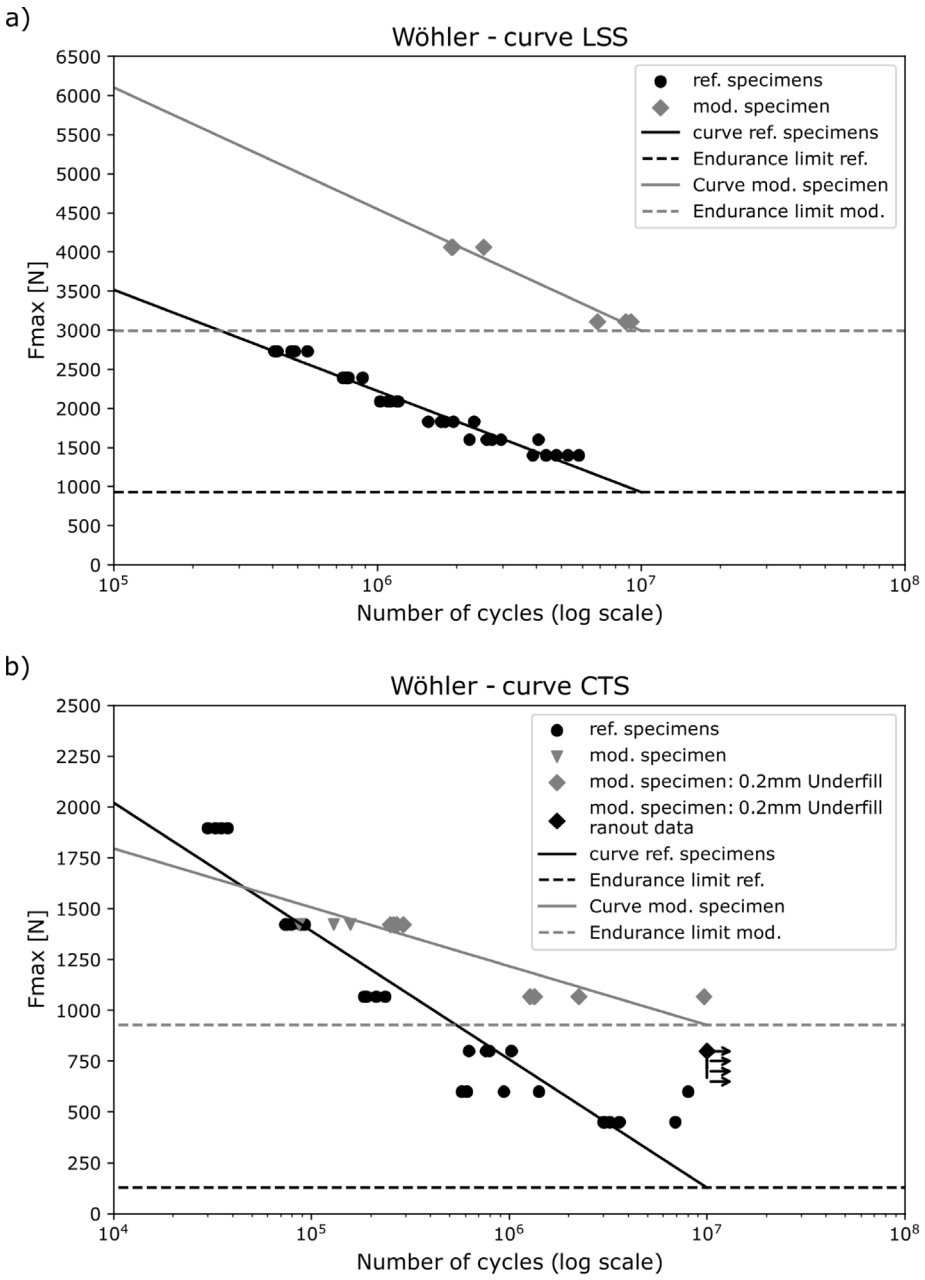

Fig. 5. Fatigue results plotted as maximum load over number of cycles (logarithmic) according to ISO 14324 of (a) lap shear samples and (b) cross tension samples.

of the spot weld, which improves the mechanical properties [29]. However, this may even be harmful as this leads to a greater strength mismatch between SZ and HAZ [30]. But since failure of the samples did not occurred within the recrystallized area of the spot weld, these differences in the microstructure are likely not to contribute to the fatigue properties.

Significant differences could be detected in the residual stress distribution in the area known to be the nucleus for fatigue cracks, the transition region between SZ and TMAZ. The resulting residual stress profile in the modified specimens are caused by the combination of the welding and locally forced forming process, where the underlying process steps are displayed in Fig. 8. Fig. 8 (a) shows the specimen before the welding process, where the initial length l_0 is defined as the distance from the edge of the pocket to the outer diameter of the shoulder. If the clamping force is now applied, Fig. 8 (b), this results in a radial elongation of the upper sheet since $l_0 < l_1+l_2$, where l_1 denotes the distance from the edge of the pocket to the outer diameter of the clamping ring and l_2 the distance from the outer diameter of the clamping ring to the outer diameter of the shoulder. The elongation is particularly significant because the increased temperature during the welding process, causes the modulus of elasticity to decrease [31]. After the welding process is completed, Fig. 8 (c), the elastic components of the locally introduced deformation leads to a spring back effect, resulting in radial compressive stresses since $l_3 < l_1+l_2$, whereas l_3 represents the distance between the outer edge of the pocket and the joined region of the spot weld, i.e. approximately the outer diameter of the shoulder. These compressive stresses are superimposed on the tensile stresses generated by the thermo-mechanical processing, in particular cooling at this stage, which leads to stress neutrality in the outer edge of the recrystallized zone.

This effect is more significant in the LSS specimen compared to the CTS specimen due to the different driving forces according to the tensile loading, influencing directly the crack path. In the LSS specimens, the crack propagates radially to the spot weld, i.e. against

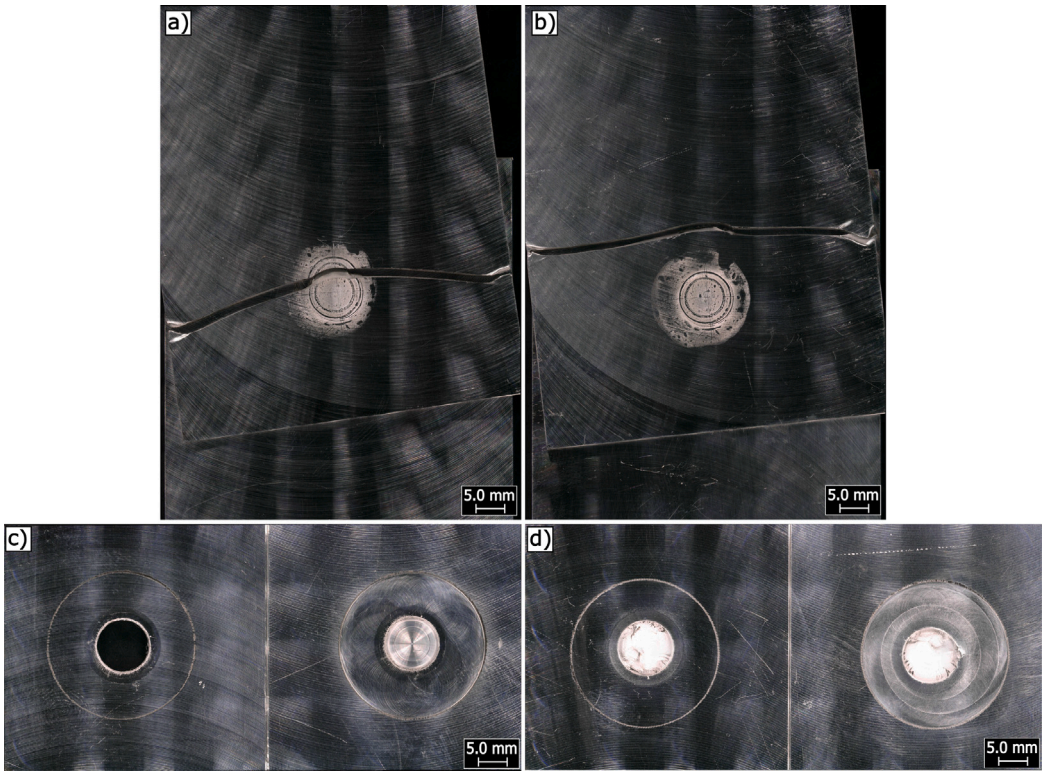

Fig. 6. Crack propagation path in (a) reference LSS sample, where the crack nucleated in transition region between SZ and TMAZ at max load of 3110 N, (b) modified LSS sample, where the crack nucleated in base material at max load of 3110 N, (c) modified CTS sample with fracture mode "pull-out" at max load of 1422 N, (d) modified CTS sample with 0.2 mm underfill, where fracture took place in the transition zone between SZ and TMAZ at max load of 1422 N.

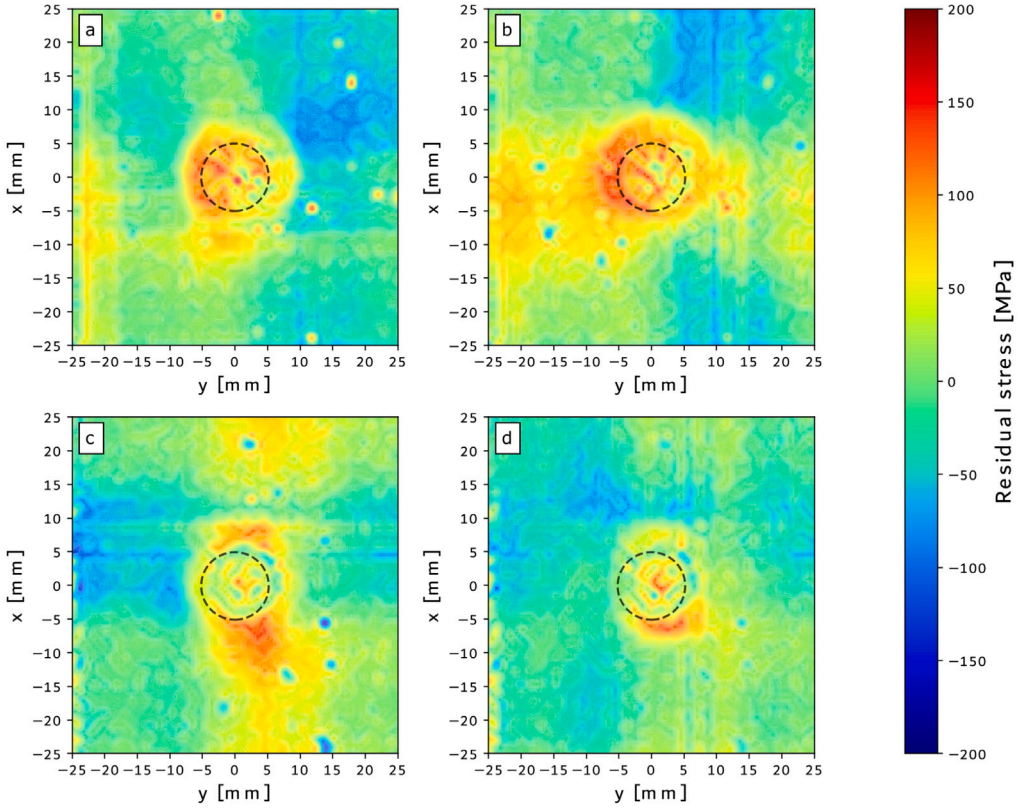

Fig. 7. Residual stresses measured in transmission: (a) σ_{xx} of the reference specimen, (b) σ_{yy} of the reference specimen, (c) σ_{xx} of the modified specimen, (d) σ_{yy} of the modified specimen.

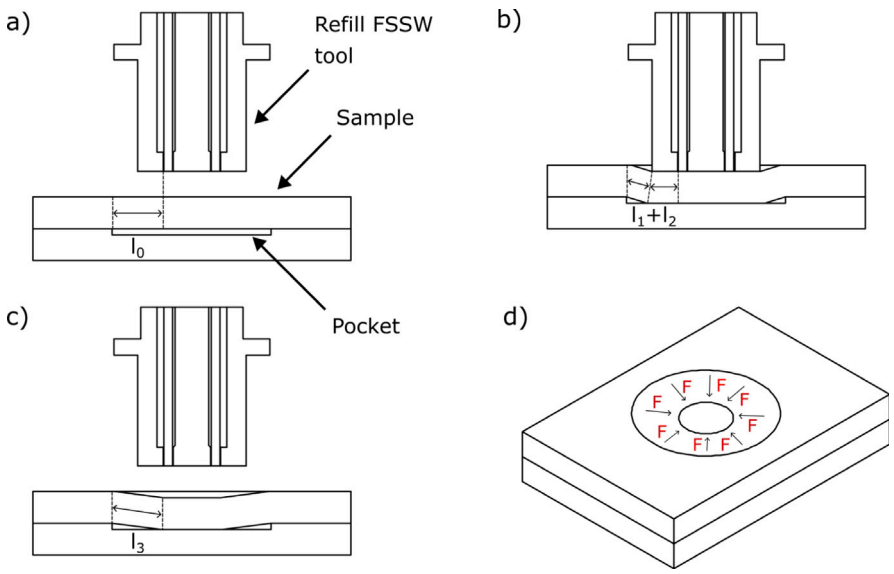

Fig. 8. Mechanism of introducing residual stresses in the modified specimens: (a) specimen before welding, (b) specimen during welding, (c) specimen after welding, (d) forces caused by the elastic springback and the change in length ratios, since $l_3 < l_1+l_2$.

the compressive stresses initiated by the deformation. Whereas in the CTS specimens the crack propagates axially to the spot weld, where compressive stresses, resulting form the locally forced forming process, are not to be expected.

In summary, in the modified LSS and CTS samples, the microstructural properties such as typical features, defects, and strength are unfavorable. Only the distribution of residual stresses is favorable for the fatigue properties, therefore the residual stresses can be named as the main influencing factor, leading to a significant improvement of fatigue properties in this work.

5. Conclusions

This study deals with one of the biggest issues of refill FSSW joints — high cycle fatigue. By specifically manipulating the residual stress distribution of the spot weld by local forming during the process, it has been possible to increase the endurance limit of shear loaded specimens by a factor of 40 and that of cross tension loaded specimens by a factor of 18. Furthermore, it could be shown that the fatigue behavior of friction stir welded joints is mainly affected by residual stresses rather than by welding defects or the microstructure. The significant increase in fatigue properties opens up new application possibilities for refill FSSW, where existing applications can be optimized.

Declaration of competing interest

The authors declare that they have no known competing financial interests or personal relationships that could have appeared to influence the work reported in this paper.

Acknowledgments

This work was executed in frame of the TTP LB project LESSMAT, funded by the German Federal Ministry for Economic Affairs and Climate Action (BMWK), project number: 03LB2021D, which is gratefully acknowledged. We also acknowledge DESY for the use of beamline P07B from Helmholtz-Zentrum Hereon.

References

[1] Shrivastava A, Krones M, Pfefferkorn FE. Comparison of energy consumption and environmental impact of friction stir welding and gas metal arc welding for aluminum. CIRP J Manuf Sci Technol 2015;9(2):159–68. http://dx.doi.org/10.1016/j.cirpj.2014.10.001.

[2] Kwee I, de Waele W, Faes K. Weldability of high-strength aluminium alloy EN AW-7475-T761 sheets for aerospace applications, using refill friction stir spot welding. Weld the World 2019;63(4):1001–11. http://dx.doi.org/10.1007/s40194-019-00732-1.

[3] Fratini L, Barcellona A, Buffa G, Palmeri D. Friction stir spot welding of AA6082-T6: Influence of the most relevant process parameters and comparison with classic mechanical fastening techniques. Proc Inst Mech Eng Part B: J Eng Manuf 2007;221(7):1111–8. http://dx.doi.org/10.1243/09544054JEM678.

[4] Allen CD, Arbegast WJ. Evaluation of friction spot welds in aluminum alloys, sae technical paper 2005-01-1252. 2005, http://dx.doi.org/10.4271/2005-01-1252.

[5] Kluz R, Kubit A, Trzepiecinski T, Faes K, Bochnowski W. A weighting grade-based optimization method for determining refill friction stir spot welding process parameters. J Mater Eng Perform 2019;28(10):6471–82. http://dx.doi.org/10.1007/s11665-019-04378-4.

[6] Zhou L, Luo LY, Wang R, Zhang JB, Huang YX, Song XG. Process parameter optimization in refill friction spot welding of 6061 aluminum alloys using response surface methodology. J Mater Eng Perform 2018;27(8):4050–8. http://dx.doi.org/10.1007/s11665-018-3472-x.

[7] Tier MD, Rosendo TS, dos Santos JF, Huber N, Mazzaferro JA, Mazzaferro CP, et al. The influence of refill FSSW parameters on the microstructure and shear strength of 5042 aluminium welds. J Mater Process Technol 2013;213(6):997–1005. http://dx.doi.org/10.1016/j.jmatprotec.2012.12.009.

[8] Li Z, Gao S, Ji S, Yue Y, Chai P. Effect of rotational speed on microstructure and mechanical properties of refill friction stir spot welded 2024 Al alloy. J Mater Eng Perform 2016;25(4):1673–82. http://dx.doi.org/10.1007/s11665-016-1999-2.

[9] Lage SBM, Campanelli LC, de Bribean Guerra AP, Shen J, dos Santos JF, da Silva PSCP, et al. A study of the parameters influencing mechanical properties and the fatigue performance of refill friction stir spot welded AlMgSc alloy. Int J Adv Manuf Technol 2019;100(1–4):101–10. http://dx.doi.org/10.1007/s00170-018-2696-0.

[10] Effertz PS, Infante V, Quintino L, Suhuddin U, Hanke S, dos Santos JF. Fatigue life assessment of friction spot welded 7050-T76 aluminium alloy using Weibull distribution. Eng Fract Mech 2016;87:381–90. http://dx.doi.org/10.1016/j.ijfatigue.2016.02.030.

[11] Becker N, dos Santos JF, Klusemann B. Experimental investigation of crack propagation mechanism in refill friction stir spot joints of AA6082-T6. Eng Fract Mech 2024;300(2):109963. http://dx.doi.org/10.1016/j.engfracmech.2024.109963.

[12] Pouget G, Reynolds AP. Residual stress and microstructure effects on fatigue crack growth in AA2050 friction stir welds. Eng Fract Mech 2008;30(3):463–72. http://dx.doi.org/10.1016/j.ijfatigue.2007.04.016.

[13] Ma YE, Staron P, Fischer T, Irving PE. Size effects on residual stress and fatigue crack growth in friction stir welded 2195-T8 aluminium – part I:

Experiments. Eng Fract Mech 2011;33(11):1417–25. http://dx.doi.org/10.1016/j.ijfatigue.2011.05.006.
[14] Bagheri B, Abbasi M, Hamzeloo R. The investigation into vibration effect on microstructure and mechanical characteristics of friction stir spot vibration welded aluminum: Simulation and experiment. Proc Inst Mech Eng Part C: J Mech Eng Sci 2020;234(9):1809–22. http://dx.doi.org/10.1177/0954406219900194.
[15] Wu M, Wu C, Gao S. Effect of ultrasonic vibration on fatigue performance of AA 2024-T3 friction stir weld joints. J Manuf Process 2017;29:85–95. http://dx.doi.org/10.1016/j.jmapro.2017.07.023.
[16] Zhang Z, Jin Y, Ma L, Ji S, Dong J, Zhao H, et al. A general strategy for achieving high-strength joining of 2024 aluminum alloys via impacting flow friction stir lap welding. A Gen Strat Achiev High- Strength Join J Manuf Process 2025;134:619–23. http://dx.doi.org/10.1016/j.jmapro.2025.01.007.
[17] Silva BH, Zepon G, Bolfarini C, dos Santos JF. Refill friction stir spot welding of AA6082-T6 alloy: Hook defect formation and its influence on the mechanical properties and fracture behavior. Mater Sci Engineering: A 2020;773:138724. http://dx.doi.org/10.1016/j.msea.2019.138724.
[18] Pettersen T, Holmedal B, Nes E. Microstructure development during hot deformation of aluminum to large strains. Met Mater Trans A 2003;34(12):2737–44. http://dx.doi.org/10.1007/s11661-003-0175-0.
[19] Chen YD, Dan CY, Shi QW, Jin L, Liu J, Chen C, et al. Influence of heating rate on the recrystallization temperature of Al–Mg alloy. J Mater Res Technol 2023;22(3):2206–11. http://dx.doi.org/10.1016/j.jmrt.2022.12.044.
[20] Svensson L-E, Karlsson L, Larsson H, Karlsson B, Fazzini M, Karlsson J. Microstructure and mechanical properties of friction stir welded aluminium alloys with special reference to AA 5083 and AA 6082. Sci Technol Weld Join 2000;5(5):285–96. http://dx.doi.org/10.1179/136217100101538335.
[21] Threadgill PL, Leonard AJ, Shercliff HR, Withers PJ. Friction stir welding of aluminium alloys. Int Mater Rev 2009;54(2):49–93. http://dx.doi.org/10.1179/174328009X411136.
[22] Bernardi M, Suhuddin UF, Fu B, Gerber JP, Bianchi M, Ostrovsky I, et al. Fatigue behaviour of multi-spot joints of 2024-T3 aluminium sheets obtained by refill Friction Stir Spot welding with polysulfide sealant. Eng Fract Mech 2023;172:107539. http://dx.doi.org/10.1016/j.ijfatigue.2023.107539.
[23] Bachmann M, Carstensen J, Bergmann L, dos Santos JF, Wu CS, Rethmeier M. Numerical simulation of thermally induced residual stresses in friction stir welding of aluminum alloy 2024-T3 at different welding speeds. Int J Adv Manuf Technol 2017;91(1–4):1443–52. http://dx.doi.org/10.1007/s00170-016-9793-8.
[24] Deplus K, Simar A, van Haver W, de Meester B. Residual stresses in aluminium alloy friction stir welds. Int J Adv Manuf Technol 2011;56(5–8):493–504. http://dx.doi.org/10.1007/s00170-011-3210-0.
[25] Brzostek RC, Suhuddin U, dos Santos JF. Fatigue assessment of refill friction stir spot weld in AA 2024–T3 similar joints. Fatigue Fract Eng Mater Struct 2018;41(5):1208–23. http://dx.doi.org/10.1111/ffe.12764.
[26] Biro AL, Chenelle BF, Lados DA. Processing, microstructure, and residual stress effects on strength and fatigue crack growth properties in friction stir welding: A review. Met Mater Trans B 2012;43(6):1622–37. http://dx.doi.org/10.1007/s11663-012-9716-5.
[27] Shen Z, Ding Y, Chen J, Fu L, Liu XC, Chen H, et al. Microstructure, static and fatigue properties of refill friction stir spot welded 7075-T6 aluminium alloy using a modified tool. Sci Technol Weld Join 2019;24(7):587–600. http://dx.doi.org/10.1080/13621718.2019.1572300.
[28] Cao JY, Wang M, Kong L, Guo LJ. Hook formation and mechanical properties of friction spot welding in alloy 6061-T6. J Mater Process Technol 2016;230:254–62. http://dx.doi.org/10.1016/j.jmatprotec.2015.11.026.
[29] Wang X, Guo M, Moliar O, Peng W, Xie C, Chen J, et al. Enhanced grain refinement and texture weakening in Al–Mg–Si alloy through a novel thermo-mechanical processing. J Alloys Compd 2022;925:166654. http://dx.doi.org/10.1016/j.jallcom.2022.166654.
[30] Zuniga SM, Sheppard SD. Determining the constitutive properties of the heat-affected zone in a resistance spot weld. Modelling Simul Mater Sci Eng 1995;3(3):391–416. http://dx.doi.org/10.1088/0965-0393/3/3/007.
[31] Tallon JL, Wolfenden A. Temperature dependence of the elastic constants of aluminum. J Phys Chem Solids 1979;40(11):831–7. http://dx.doi.org/10.1016/0022-3697(79)90037-4.